

An optimized snowmelt lysimeter system for monitoring melt rates and collecting samples for stable water isotope analysis

Andrea Rücker^{1,2*}, Massimiliano Zappa¹, Stefan Boss¹, Jana von Freyberg^{2,1}

¹ Swiss Federal Institute for Forest, Snow and Landscape Research (WSL), Zürcherstrasse 111, 8903 Birmensdorf, Switzerland.

² Department of Environmental Systems Science, ETH Zurich, Universitätsstr. 16, 8092 Zurich, Switzerland.

* Corresponding author. Tel.: +41 44 739 2487 or +41 44 6329 171. Fax: +41 44 7392 215. E-mail: andrea.ruecker@wsl.ch

Abstract: The contribution of snow meltwater to catchment streamflow can be quantified through hydrograph separation analyses for which stable water isotopes (^{18}O , ^2H) are used as environmental tracers. For this, the spatial and temporal variability of the isotopic composition of meltwater needs to be captured by the sampling method. This study compares an optimized snowmelt lysimeter system and an unheated precipitation collector with focus on their ability to capture snowmelt rates and the isotopic composition of snowmelt. The snowmelt lysimeter system consists of three individual unenclosed lysimeters at ground level with a surface of 0.14 m^2 each. The unheated precipitation collector consists of a 30 cm-long, extended funnel with its orifice at 2.3 m above ground. Daily snowmelt samples were collected with both systems during two snowfall-snowmelt periods in 2016. The snowmelt lysimeter system provided more accurate measurements of natural melt rates and allowed for capturing the small-scale variability of snowmelt process at the plot scale, such as lateral meltwater flow from the surrounding snowpack. Because of the restricted volume of the extended funnel, daily melt rates from the unheated precipitation collector were up to 43% smaller compared to the snowmelt lysimeter system. Overall, both snowmelt collection methods captured the general temporal evolution of the isotopic signature in snowmelt.

Keywords: Snowmelt lysimeter; Snowmelt collection; Snowmelt rate; Stable water isotopes.

INTRODUCTION

Snowpacks in mountainous headwater catchments comprise important freshwater resources in many regions of the world (Stewart, 2009). In Switzerland, about 42% of river discharge is fed by snow meltwater (Zappa et al., 2012), so that hydropower production strongly depends on the seasonal water storage in higher elevations (Beniston, 2003). In some mountainous snow-dominated regions, predicted effects of climate change, such as higher air temperatures and lower precipitation rates, will result in decreasing snow volumes, as well as in earlier and shortened snowmelt (Barnett et al., 2005; Beniston, 2003; Berghuijs et al., 2014). Hereby, the mid and lower altitudes will be affected the most by changes in water storage (Barnett et al., 2005), because the snowline rises about 150 m in elevation with every of 1°C increase in air temperature (Beniston, 2003). By the end of the 21st century, mountainous catchments in Switzerland are expected to receive up to 50% less snow at 2000 m a.s.l. and up to 90% less snow at about 1000 m a.s.l. (Beniston, 2003). As a consequence, the risk for summer low flows in downstream valleys is likely to increase (Stewart, 2009).

In order to adapt water management strategies to future changes in the hydrological cycle, the physical mechanisms that control streamflow generation from snowmelt, have to be understood (Bierkens and van Beek, 2009; Šanda et al., 2010; Singla et al., 2012; Staudinger and Seibert, 2014).

Environmental tracers, such as stable water isotopes (^{18}O , ^2H), can be used to identify water sources that contribute to river streamflow (Klaus and McDonnell, 2013). In the last decades, stable water isotopes have been applied in hydrograph separation analyses to quantify the contribution of snowmelt to catchment outflow (Ala-aho et al., 2017; Dinçer et al., 1970; Hooper and Shoemaker, 1986; Huth et al., 2004; Laudon, 2004; Penna et al., 2014b; Rodhe, 1998; Šanda et al., 2014; Taylor et al., 2002b). Hereby, the isotope signal of snowmelt can be

highly variable in time during individual melt periods similar to the short-term isotopic evolution of liquid precipitation (Munksgaard et al., 2012; von Freyberg et al., 2017). This isotopic variability in snowmelt is driven by mixing with incoming precipitation (rain or snow), snow redistribution by wind, and isotopic fractionation of snowmelt during (re-)freezing and condensation in the snowpack (Ala-aho et al., 2017; Cooper, 1998; Lyon et al., 2010; Rodhe, 1998; Taylor, 2001; Unnikrishna et al., 2002).

During rain-on-snow events, rainwater can mix with the snow and thus significantly change the isotopic composition of melt from the snowpack (Juras et al., 2016; Penna et al., 2014a; Unnikrishna et al., 2002). In addition, the snowpack becomes progressively isotopically enriched during the melt-out, which is directly linked to the rate of snowmelt (Ala-aho et al., 2017; Hooper and Shoemaker, 1986; Laudon, 2004; Lee et al., 2010; Taylor et al., 2001; Unnikrishna et al., 2002).

In order to use stable water isotopes of snowmelt for hydrograph separation analyses, the spatial and temporal variability of the isotopic composition of meltwater needs to be captured by the sampling method (Earman et al., 2006; Laudon et al., 2002; Schmieder et al., 2016; Taylor et al., 2002b). In addition, snowmelt rates have to be recorded to volume-weight the isotope values of composite samples.

Different methods exist to measure the snowmelt rates and to collect samples for isotope analysis. Snowmelt can be collected, for instance, from the base of a snow pit (Taylor et al., 2002b) or from soil cores (Frisbee et al., 2010). In remote and mountainous terrain, these manual methods are often the only possibility to obtain snowmelt samples, however, sample collection in such catchments is laborious, can be dangerous and may be prone to sampling errors. An alternative method for direct meltwater collection is a passive capillary sampler to capture an integrated meltwater sample throughout the melt season (Frisbee et al., 2010; Penna et al., 2014a). For more

frequent sampling, a melt pan can be installed beneath a snowpack from which meltwater drains through a pipe into a sample collector (Bales et al., 1993; Taylor et al., 2001). Alternatively, an unheated precipitation collector can be deployed to sample snowmelt (Earman et al., 2006; Gröning et al., 2012). Two different types of unheated precipitation collectors were evaluated by Earman et al. (2006) by collecting six-month bulk snowmelt for subsequent isotope analysis. The unheated precipitation collectors were designed to capture the snowmelt composition at 1 m above ground by using extension tubes on top of the 10 cm-diameter funnels. The extension tubes of the two systems were 7.5 cm (regular funnel) and 15 cm long (extended funnel) respectively. Earman et al. (2006) found that the samples from the collector with the extended funnel were “[...] more representative of infiltration water isotope composition than a fresh snow sample because the snow in the extended collector is subject to many of the snow metamorphism effects that impact snow on the ground.” To test whether accelerated melt caused isotope effects in the snowmelt sample, two of the extended funnel precipitation collectors were painted in either black or white colour (Earman et al., 2006). However, the colouring of the funnel was not found to significantly affect the isotopic composition of the bulk melt sample (Earman et al., 2006). Hence, the extended funnel collector might be a suitable method for collecting a sample that is representative for the isotopic composition of the snowpack. Rates of snowmelt are, however, likely to remain highly uncertain due to under-catch and wind drift (Rasmussen et al., 2012).

Snowmelt lysimeters provide another approach to combine the measurements of snowmelt rates and the collection of snowmelt samples. Snowmelt lysimeters were primarily developed to measure only snowpack outflow for the evaluation of snowmelt process representations in snowmelt modelling studies (Haupt, 1969; Kattelmann, 2000; Martinec, 1987; Obled and Rosse, 1977; Würzer et al., 2017). The first systems were developed at the Central Sierra Snow Laboratory in the 1950s and were commonly applied since the late 1970s (e.g., Helvey and Fowler, 1980; Kattelmann, 2000; Martinec, 1987; Shanley et al., 1995; Tekeli et al., 2005). Further technical improvements of snowmelt lysimeter systems enabled the collection of meltwater samples for subsequent isotope analysis (Herrmann, 1978; Laudon, 2004; Unnikrishna et al., 2002).

Originally, a snowmelt lysimeter consists of a collector that traps meltwater flowing out of the snowpack. The collector is connected by a tube or conduit to a flow-recording device (Kattelmann, 2000; Tekeli et al., 2005). There exist two types of snowmelt lysimeters that are (i) enclosed with high barriers (extending the maximum snow depth to create an isolated snow column that only drains into the melt outlet), or (ii) unenclosed with a short rim above the base (usually 10–50 cm). In natural systems, however, the enclosed system is difficult to build and to operate and therefore, unenclosed snowmelt lysimeters are commonly deployed (Kattelmann, 2000). A major disadvantage of unenclosed lysimeters is the spatial variability of melt rates due to lateral inflow of meltwater from the surrounding snowpack (Kattelmann, 2000; Unnikrishna et al., 2002). For this reason, a set of at least three individual unenclosed snowmelt lysimeters is recommended to capture the spatio-temporal variability of melt processes at a sampling location (Kattelmann, 2000). In the past, melt rates were recorded quasi-continuously with tipping buckets (e.g., Bales et al., 1993; Juras et al., 2016; Taylor et al., 2001) or continuously with water level recorders (e.g., Haupt, 1969; Herrmann, 1978). Most studies integrated melt rate measurements from several locations, while samples for isotope analysis were generally obtained from only one

meltwater collection system (Lee et al., 2010; Taylor et al., 2001; Unnikrishna et al., 2002). Occasionally, melt water sampling for subsequent isotope analysis was adjusted to capture individual melt events at a high temporal resolution, however, regular meltwater sampling over the entire period with snow cover was rarely done (Hooper and Shoemaker, 1986; Schmieder et al., 2016; Taylor et al., 2001).

Based on snowmelt lysimeter measurements, a recent study successfully simulated the spatiotemporal variability of the isotopic composition of snowmelt at the catchment scale by considering fractionation processes in the snowpack and different landscape characteristics (Ala-aho et al., 2017). The isotope signature of the meltwater leaving the snowpack during rain-on-snow events could, however, not be represented adequately because the model assumes complete mixing in the snowpack (Ala-aho et al., 2017). In addition, the transferability of the model to catchments with different landscape characteristics (i.e., elevation, slope, vegetation) is limited, because only a few snowmelt collection systems exist worldwide that sample snowmelt at high temporal resolution and at different locations during the entire snow cover period.

So far, snowmelt lysimeters are among the most sophisticated meltwater collection systems, although their application is often technically complicated and cost-intensive. Thus, we designed a fully automated snowmelt lysimeter system (for snowmelt sampling and melt rate monitoring) based on standard technical components, which can potentially be rebuilt at other sites with moderate effort and costs.

Alternative low-cost methods, such as unheated extended funnel collectors may also be suitable to capture melt rates and meltwater isotopic composition, especially in remote areas. To the best of our knowledge, a detailed comparison of the two sampling methods has not yet been carried out. Therefore, the objective of the present study was to present a detailed evaluation of the optimized snowmelt lysimeter systems with regard to the measured snowmelt rates and the isotopic composition of snowmelt. In addition, the functionality of the unheated precipitation collector with extended funnel as a low-cost alternative to a lysimeter system was tested. Both snowmelt collection systems were installed at a grassland site in a pre-alpine catchment in central Switzerland. The comparison was carried out based on measurements during two individual snowfall-snowmelt periods in April and November 2016.

METHODOLOGY

Field site

The snowmelt lysimeter system and the unheated precipitation collector with extended funnel were installed at the field site Erlenhöhe (1216 m a.s.l.), which is located in the central Swiss pre-Alps in the hydrological research catchment Erlenbach (Burch et al., 1996; Hegg et al., 2006). The catchment vegetation is dominated by forests (53%), while 22% of the area is partly-forested and 25% is covered with grassland (Fischer et al., 2015). The bedrock is composed of Flysch, a calciferous tertiary sediment with limited permeability (Burch et al., 1996).

A meteorological station at the field site Erlenhöhe provides measurements of climatological parameters, such as air temperature and snow depth at 10-minute temporal resolution (Stähli and Gustafsson, 2006). Incoming precipitation is measured with a heated rain gauge at 1.50 m above ground. This rain gauge did not allow for sample collection, and thus in this study it was used only to provide reference measurements for incoming precipitation. Average annual precipitation at the site is

2300 mm/y (Feyen et al., 1999) from which around one-third falls as snow (Stähli and Gustafsson, 2006). Average air temperature is 6°C with its minimum in February (-2°C) and its maximum in August (17°C) (Feyen et al., 1999).

Snowmelt collection

Snowmelt lysimeter system

An unenclosed snowmelt lysimeter system was developed to measure melt rates at 1-minute temporal resolution and to sample meltwater at daily temporal resolution over an area of approximately 3x4 m (Figure 1). The snowmelt lysimeter system consists of three PE-HD funnels (each 0.14 m² in diameter) with rims of 5.9 cm, that were each located above a tipping bucket (ECRN-100 High-Resolution Rain Gauge, Decagon Devices Inc., Pullman (WA), USA). The tipping bucket recorded melt rates at 5 ml volume increments (i.e., 0.04 mm m⁻²) with a measurement uncertainty of 10%. To avoid freezing in the mechanism of the tipping bucket, a 12 W heating patch (110 mm x 77 mm) was attached to the inside wall of the rain gauge funnel. The meltwater drains from each funnel by gravity through a silicon tube (ca. 3–4° gradient, diameter 10x14 mm) to its respective PE-HD 10 l vessel. The vessels were situated in a watertight metal container embedded in the ground downhill of the lysimeter funnels.

Once a day at 05:40, the snowmelt samples were pumped individually from each vessel by an automatic water sampler equipped with 24 bottles (April 2016 period: 6712-Fullsize Portable Sampler, Teledyne Isco, Lincoln (NE), USA, November 2016 period: Maxx P6L – Vacuum System, Maxx GmbH, Rangendingen, Germany). Because only one automatic water sampler was used during each period, the connection between the vessels and the pumping tube of the automatic water sampler was controlled through pinch solenoid valves (ASCO Numatics Sirai Srl, Bussero, Italy), operated by a Datalogger (CR-1000, Campbell Scientific, Loughborough, Great Britain). Up to 300 ml was pumped from each collection vessel into one separate dry 1 l bottle in the automatic water sampler.

After each pump cycle, remaining water in the suction tube was blown back into the sampled vessel to reduce carry-over effects. After all three vessels were samples (ca. 20 min), pinch solenoid valves situated at the outlets of the vessels were opened simultaneously to release the remnant water through an outlet pipe. The 6 m long outlet pipe ran downhill of the lysimeter system which allowed for free drainage of the vessels without tailback. At 06:00, the valves at the outlets of the vessels were closed again and meltwater collection started for the next 1-day sampling period. Once a week, the filled sample bottles of the automatic water sampler were replaced with empty bottles. The filled sample bottles were sealed with lids to avoid leakage during the transport to the laboratory.

A webcam (Webcam ROLINE RBOF4-1 Bullet IP 4MP, Secomp, Bassersdorf, Switzerland) took hourly pictures of the snowmelt lysimeter system, which allowed for documenting the timing of snowfall and melt. The snowmelt lysimeter system and the webcam were connected to the local power grid. This set-up of the snowmelt lysimeter system cost around 4000 US\$ (excluding the webcam and the automatic water sampler).

Unheated precipitation collector with extended funnel

For the unheated precipitation collector, we used the basic parts of the “Palmex” collector (Palmex d.o.o., Zagreb, Croatia), such as the plastic funnel (13.5 cm in diameter) and the extended aluminium funnel (15 cm diameter, 30 cm long), which was installed on top of the plastic funnel (Figure 2) (Gröning et al., 2012). The extended funnel was modified by painting it with black colour to accelerate the snowmelt of the accumulated snow and thus prevent evaporative fractionation effects of the meltwater sample in the funnel (Earman et al., 2006). This set-up of the unheated precipitation collector cost around 200 US\$.

The unheated precipitation collector was installed at the field site at Erlenhöhe so that the orifice of the extended funnel was at a height of 2.3 m above ground. With this set-up, the unheated precipitation collector sampled a mixture of liquid precipitation,

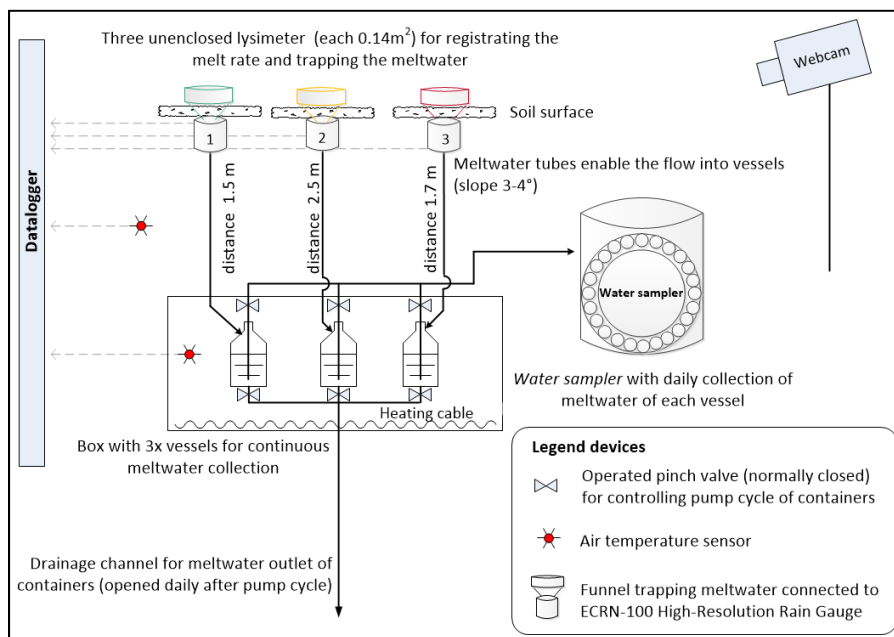


Fig. 1. Set-up of the snowmelt lysimeter system at the field site Erlenhöhe on a 3 m x 4 m area. Three funnels (1, 2 and 3) collect snowmelt which is draining through silicon tubes to the three collection vessels. The data logger controls three pinch valves to pump the meltwater into sample bottles of an automatic water sampler. Remnant meltwater in the vessels is released simultaneously to the drainage pipe after each pump cycle by opening the three valves at the outlets of the collection vessels (see also Figure A1 and Figure A2).

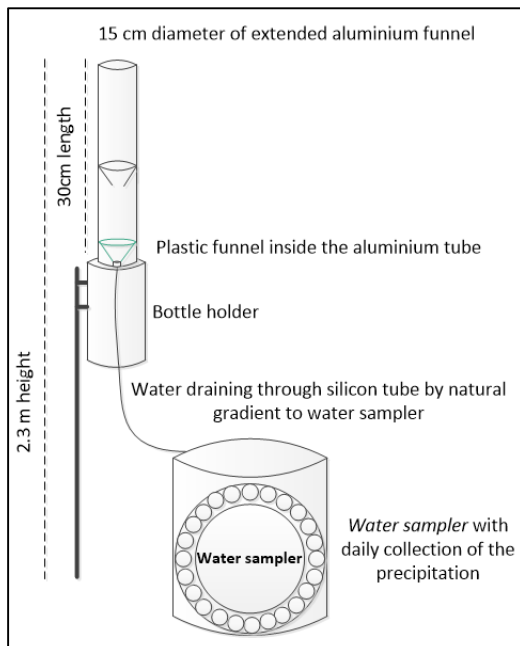


Fig. 2. Set-up of the unheated precipitation collector with extended funnel connected to an automatic water sampler installed at Erlenhöhe. The meltwater drains by gravity to the automatic water sampler (see also Figure A3).

snow and snowmelt. Despite the black-coloured funnel, fractionation of the snow sample in the funnel of the unheated precipitation collector might still occur when meltwater refreezes, depending on ambient air temperature and incoming solar radiation.

The meltwater samples from the unheated precipitation collector drained by gravity into a dry HDPE sample bottle in an automatic water sampler (6712-Fullsize Portable Sampler, Teledyne Isco, Lincoln (NE), USA), that was connected to the local power grid. Every day at 05:40, the automatic water sampler rotated the injection arm to a new sample bottle. Since these sample bottles were replaced in a 3-weeks cycle, the bottles were modified to reduce evaporation and isotopic fractionation. This was done by plugging a 100 ml syringe housing (i.e., without piston) into the opening of the sample bottle in order to avoid evaporation and isotopic fractionation. For the collection and transport of the samples, the 1 l sample bottles were sealed with a lid to avoid leakage. In the laboratory, the meltwater sample volumes were determined by weighting the filled sample bottles and subtracting the known weights of the empty sample bottles.

Isotope analysis

Until sample preparation for isotope analysis, the samples from both collection systems remained sealed and refrigerated at 4°C. Prior to analysis, all water samples were melted at room temperature, if necessary, filtrated through 0.45- μm Teflon filters (DigiFilter micron Teflon) and filled into 2-ml glass vials. The water samples were analysed for the stable water isotopes (^{18}O , ^2H) by laser spectroscopy (Los Gatos Research, Isotopic Water Analyzer LGR IWA-45-EP; ABB Los Gatos Research, San Jose, California, USA.) at the laboratory of the Swiss Federal Institute for Forest, Snow and Landscape Research (WSL). The measurement precision of the analyser was 0.5‰ for $\delta^{18}\text{O}$ and 1.0‰ for $\delta^2\text{H}$. Isotopic abundances are reported through the δ notation relative to the IAEA-VSMOW-II standards.

Comparison analysis

Two snowfall periods with subsequent snowmelt were monitored between 24 April and 2 May 2016 (referred to as April period), as well as between 6 and 22 November 2016 (referred to as November period). Because the duration and depth of snow cover were different for these two periods, they provided ideal data sets to compare the snowmelt lysimeter system and the unheated precipitation collector with regard to melt rates (daily temporal resolution), timing of melt and the isotopic composition of the daily meltwater samples. In addition, total volumes of incoming precipitation (rain and snowmelt) captured by both collection systems during the April and November periods were compared with the measurements (rain and snow) of the heated rain gauge.

The three individual lysimeters of the snowmelt lysimeter system allowed for analysing the spatial variations in snowmelt and its isotopic composition at the plot scale. For this, the 1-minute melt rate recordings of the tipping buckets underneath each individual lysimeter were aggregated to 10-minute sums for easier comparison. Additionally, the peak times during six melt events during the April period (SM-April-a-b-c) and the November period (SM-Nov-a-b-c) were calculated. Peak times were defined as the time of the highest 10-minute melt rate during a melt event.

RESULTS

For both snowfall periods in April and November 2016, the initial snowpacks were established during high-intensity rainfall event that became snowfall when air temperature decreased (Figure 3a, Figure 4a). During the April period, the snowpack started to build up on 23 April 21:00 and was completely melted on 30 April 13:00, i.e. the snow cover lasted for about seven days. During that period, individual snowfall events occurred that started on 24 April 20:00 and on 26 April 22:00, respectively, resulting in maximum snow depths of around 30 cm. On 1 May 00:30, a small snow pack (5 cm) was built up again that lasted until 2 May 01:30. Because this event occurred after the continuous snowpack was completely melted, the cumulative sum of total melt during the April period was calculated from 23 April 21:00 to 30 April 13:00.

The snowpack during the November period lasted from 6 November 08:20 to 22 November 09:30, and thus seven days longer than that of the April period (Figure 4a). The maximum snow depth of 44 cm was reached on 12 November 03:00, after air temperature decreased during a heavy precipitation event that started on 11 November 02:10. During the melt-out, the snowpack increased again by 3 cm on 19 November because of another precipitation event with a mixture of rain and snow (19 mm).

Comparison of the two snowmelt collection systems with regard to total precipitation and snowmelt volumes

The cumulative sums of meltwater collected with the heated rain gauge, the unheated precipitation collector, the three individual snowmelt lysimeters, as well as the snowmelt lysimeter system (i.e., the average of the three individual lysimeters) during the April and November periods are presented in Table 1, as well as in Figure 3b.

For the April period, the heated rain gauge recorded 61.1 mm incoming precipitation (rain and snow). The individual snowmelt lysimeters recorded slightly larger volumes of snowmelt and rain that were between 62.3 and 73.4 mm. The average value for the entire snowmelt lysimeter system was

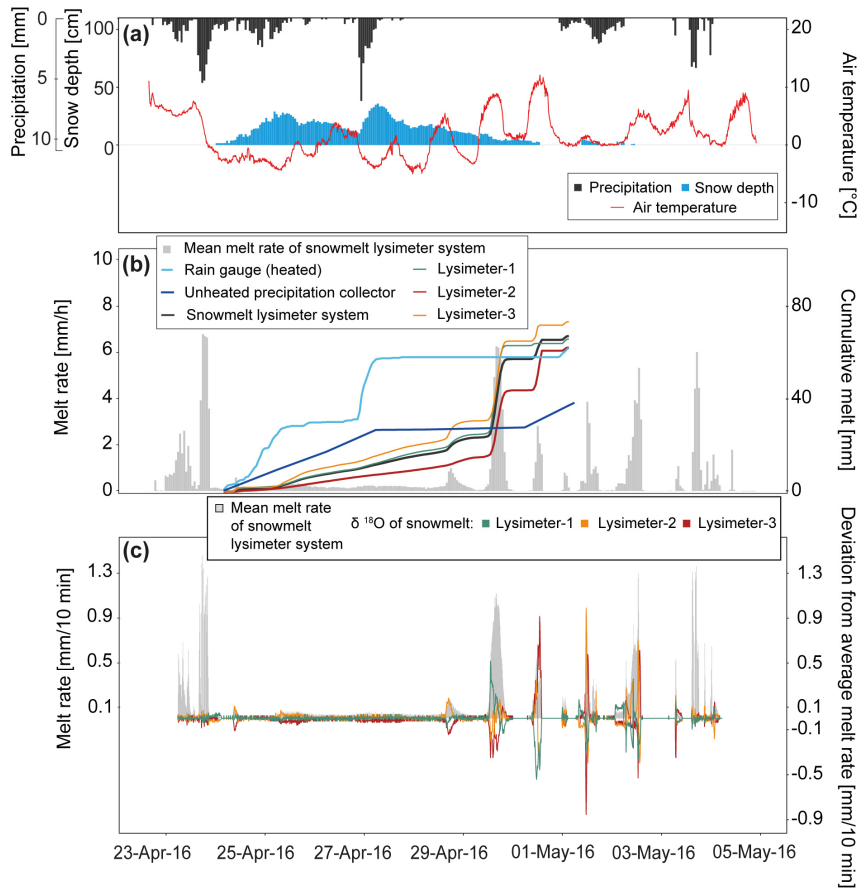


Fig. 3. The snowfall-snowmelt period in April 2016. (a) Precipitation and snow depth (left axis) and air temperature (right axis) at the field site Erlenhöhe. (b) Melt rates measured with the snowmelt lysimeter system (left axis), their cumulative sum (calculated from the mean of the three individual lysimeters), as well as the cumulative sum of the three individual lysimeters, the unheated precipitation collector and the heated rain gauge (right axis). (c) 10-minute aggregated melt rates of the snowmelt lysimeter system (left axis) and the absolute difference from the mean for each individual lysimeter (right axis).

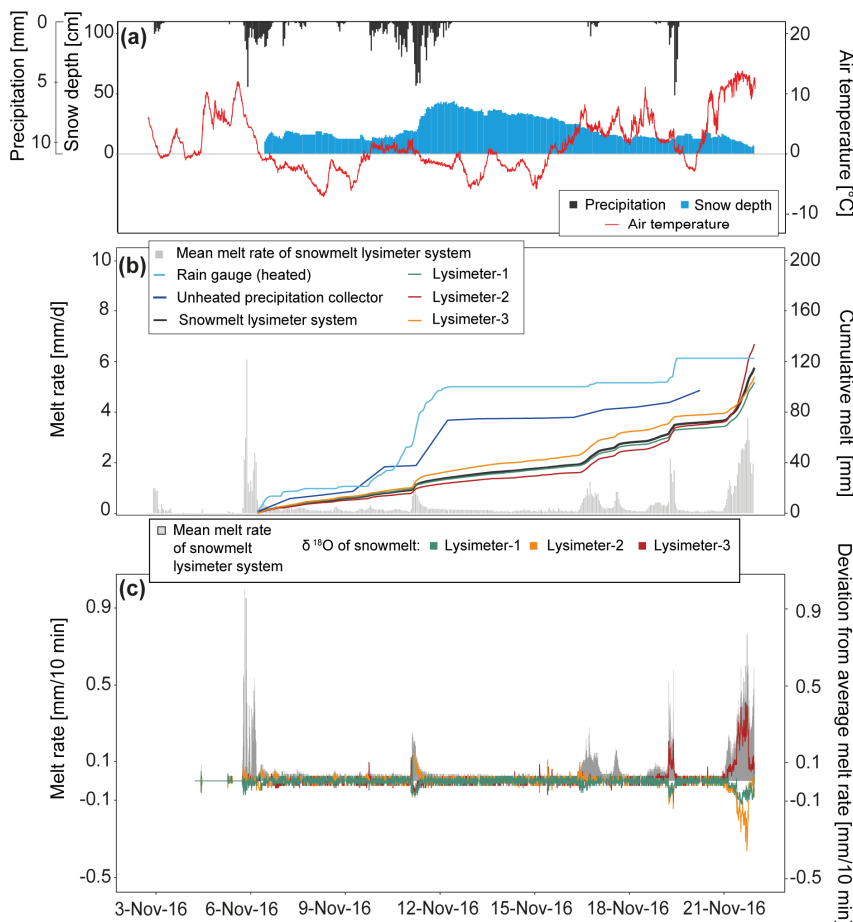


Fig. 4. The snowfall-snowmelt period in November 2016. (a) Precipitation and snow depth (left axis) and air temperature (right axis) at the field site Erlenhöhe. (b) Melt rates measured with the snowmelt lysimeter system (left axis), their cumulative sum (calculated from the mean of the three individual lysimeters), as well as the cumulative sum of the three individual lysimeters, the unheated precipitation collector and the heated rain gauge (right axis). (c) 10-minute aggregated melt rates of the snowmelt lysimeter system (left axis) and the absolute difference from the mean for each individual lysimeter (right axis).

Table 1. Cumulative snowmelt during the April and November period in 2016 recorded with the three individual snowmelt lysimeters, the snowmelt lysimeter system (mean of the three individual snowmelt lysimeters; incl. standard error) and the unheated precipitation collector. The total amount of precipitation measured with a heated rain gauge is included for comparison.

	Total snowmelt and precipitation [mm]	
	24–30 April	6–22 November
Lysimeter-1	65.8	110.1
Lysimeter-2	62.3	151.4
Lysimeter-3	73.4	120.6
Snowmelt lysimeter system (mean \pm std. error)	67.2 \pm 3.3	127.4 \pm 12.4
Unheated precipitation collector	38.4	97.2
Heated rain gauge (rain and snow)	61.1	121.2

67.2 \pm 3.3 mm (mean \pm standard error), and thus 9% larger than the measurement of the heated rain gauge. The total amount of meltwater and rain registered by the unheated precipitation collector was 38.4 mm, which was much lower (37%) than that of the measurement of the heated rain gauge.

For the November period, total incoming precipitation (rain and snow) measured with the heated rain gauge was 121.2 mm. In comparison, the three individual lysimeters recorded values between 110.0 mm and 151.4 mm, with the average value of 127.4 \pm 12.4 mm, i.e. 5% more than what was recorded by the heated rain gauge. The unheated precipitation collector (97.2 mm) underestimated total precipitation (rain and melt) by 20% relative to the heated rain gauge.

Figures 6a,c and Figures 7a,c show the daily melt rates measured with the snowmelt lysimeter system and the unheated precipitation collector. No comparison was made to the heated rain gauge because it did not measure melt from a snowpack. Overall, the melt rates recorded with the unheated precipitation collector were smaller than those of the snowmelt lysimeter system, except for the times when the initial snowpack was built up (24–27 April and 6–7 November, 10 and 12 November). For instance, on 10 and 12 November, the unheated precipitation collector recorded 19 mm and 36 mm of snowmelt, while only 6 mm and 3 mm of snowmelt was registered by the

snowmelt lysimeter system, respectively. During the melt-out of the snowpack, the snowmelt lysimeter system recorded substantially more snowmelt than the unheated precipitation collector, such as on 29 April (34 mm and 0 mm, respectively) and 21 November (50 mm and 0 mm, respectively).

Stable water isotopes in precipitation and snowmelt

The $\delta^{18}\text{O}$ and $\delta^2\text{H}$ values of the snowmelt samples collected with both the snowmelt lysimeter system and the unheated precipitation collector were highly correlated with each other (R^2 better than 0.98), and therefore the following analysis is based on the $\delta^{18}\text{O}$ values only. The respective figures showing the $\delta^2\text{H}$ values are presented in the supplementary material (Figure A4, Figure A5). During the April period, the $\delta^{18}\text{O}$ values of the samples from the unheated precipitation collector ranged from -14.5‰ to -6.9‰ , while the $\delta^{18}\text{O}$ values of the snowmelt lysimeter-based samples were between -16.5‰ and -11.5‰ (Figures 6b,c). During the November period, the meltwater samples were isotopically lighter than during the April period, with $\delta^{18}\text{O}$ values ranging between -22.6‰ and -9.9‰ for the unheated precipitation collector, and between -23.5‰ and -13.8‰ for the snowmelt lysimeter system (Figures 7b,c). On average, the meltwater samples from the unheated precipitation collector were isotopically heavier than those from the snowmelt lysimeter system (i.e. average difference of by 3.2% and 2.5% for the April and November periods, respectively). For both snowmelt collection systems, the temporal variability of $\delta^{18}\text{O}$ between the daily meltwater samples shows a distinct decrease in $\delta^{18}\text{O}$ at the beginning of the snowfall (i.e. for the lysimeter system: until 25 April by -4.3‰ , 2 May by -2.9‰ and 7 November by -5.6‰ , Figures 6b,c and Figures 7b,c). This decrease in $\delta^{18}\text{O}$ is followed by a slower increase until the complete melt-out of the snowpack. This general temporal pattern of stable isotopes in snowmelt was captured by both sampling systems, the unheated precipitation collector and the snowmelt lysimeter system. In addition, the three individual snowmelt lysimeters captured a very similar isotopic signature of the snowmelt over time (Figure 6c and Figure 7c). The meltwater $\delta^{18}\text{O}$ values from the unheated precipitation collector showed a larger short-term variability (e.g., 28 April, 10 and 17 November), as well as a one-day time shift relative to the snowmelt lysimeter system.

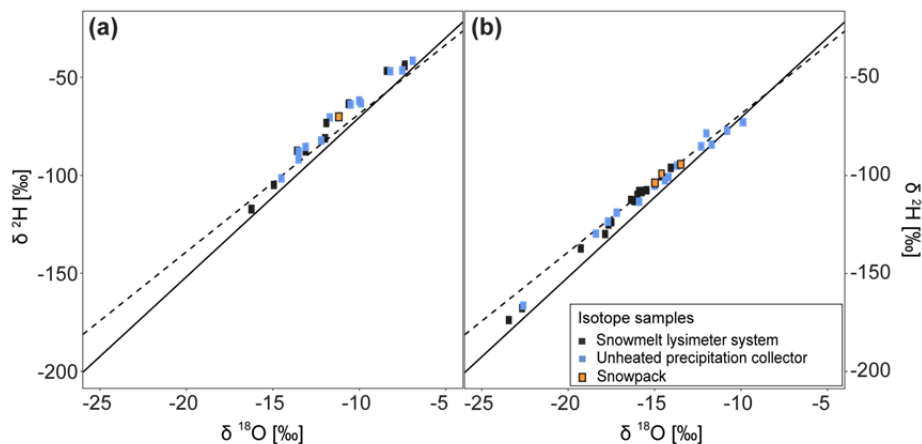


Fig. 5. Dual isotope plots for the April and November period showing the isotopic composition of the samples collected with the snowmelt lysimeter system (black) (i.e., average of the three individual lysimeters) and the unheated precipitation collector (blue). Bulk snow samples that were collected manually at weekly intervals at the field site are shown for comparison (orange). The global meteoric water line after Clark and Fritz (1997) is: $\delta^2\text{H} = 8.13 * \delta^{18}\text{O} - 10.8$ (solid black line). The linear regression line is $\delta^2\text{H} = 7.04 * \delta^{18}\text{O} - 1.75$ (dashed black line) and was obtained from rainwater samples collected at the field site in Erlenhöhe during the snow-free seasons (May till October) in 2016 and 2017.

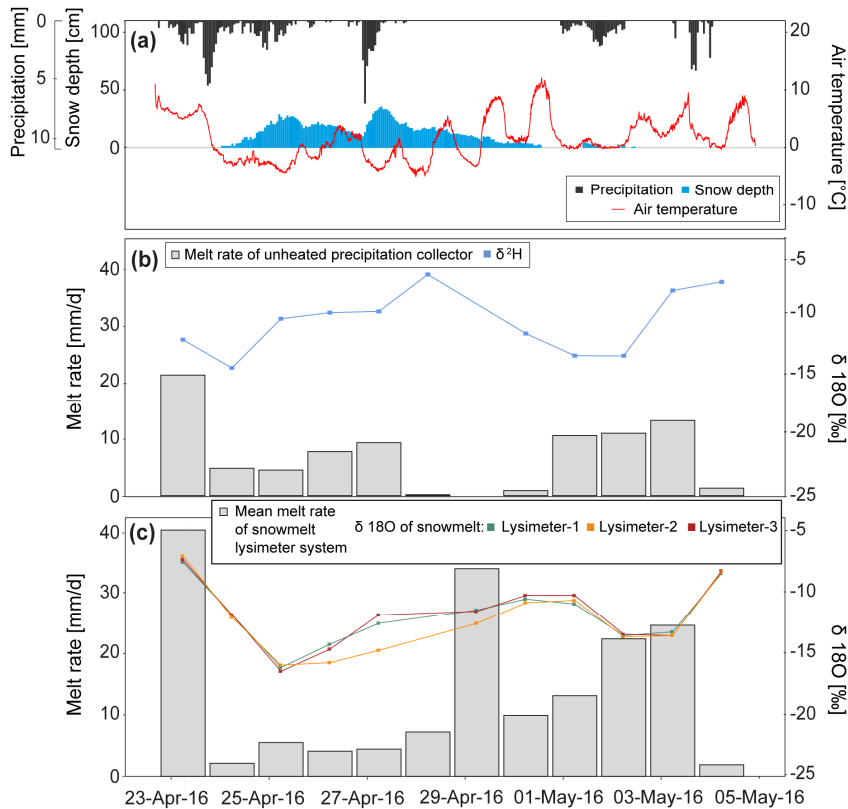


Fig. 6. The snowfall-snowmelt period in April 2016. (a) Precipitation and snow depth (left axis) as well as air temperature (right axis) at the field site Erlenhöhe. (b) Daily meltwater sample volume (left axis) and their $\delta^{18}\text{O}$ (right axis) from the unheated precipitation collector with extended funnel values. (c) Daily meltwater sample volume (left axis) and $\delta^{18}\text{O}$ values (right axis) from the snowmelt lysimeter system.

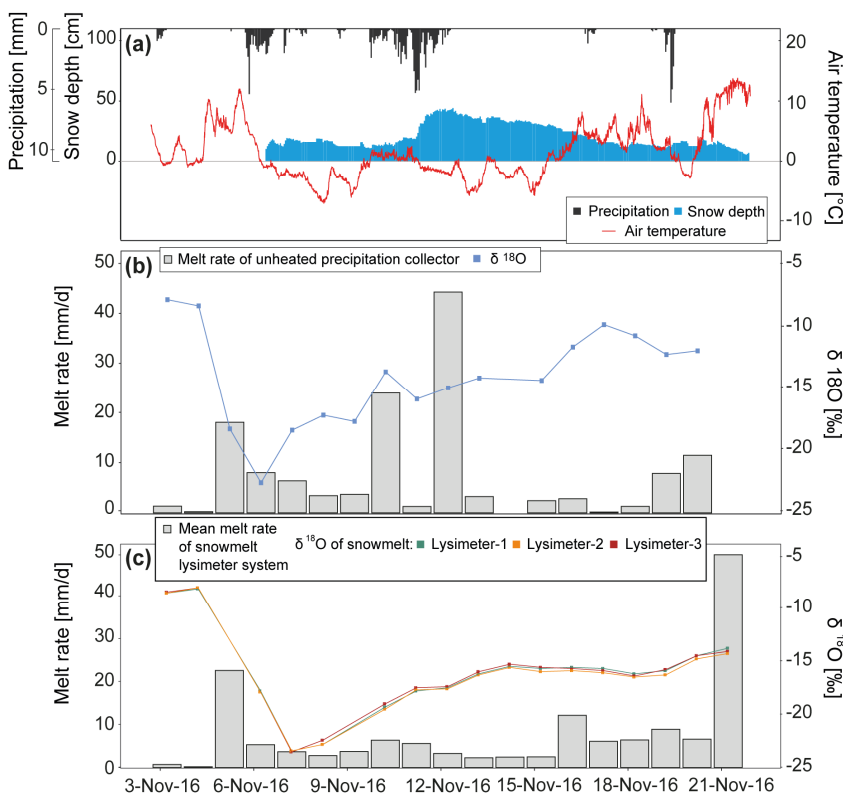


Fig. 7. The snowfall-snowmelt period in November 2016. (a) Precipitation and snow depth (left axis) as well as air temperature (right axis) at the field site Erlenhöhe. (b) Daily meltwater sample volume (left axis) and their $\delta^{18}\text{O}$ (right axis) from the unheated precipitation collector with extended funnel values. (c) Daily meltwater sample volume (left axis) and $\delta^{18}\text{O}$ values (right axis) from the snowmelt lysimeter system.

In the dual isotope space, most of the meltwater samples from both sampling systems plot on the linear regression line (Figure 5). This linear regression line, which was obtained from rainwater samples collected at the same field site during the snow-free seasons (May till October) in 2016 and 2017, is used

here as first approximation of the local meteoric water line. Except for the three most negative meltwater samples of the November period (Figure 5b), none of the meltwater samples plot substantially below the linear regression line.

Table 2. Temporal variation of melt rates and melt volumes measured with the three individual lysimeters during six melt events in April (SM-April-a-b-c) and November (SM-Nov-a-b-c) in 2016. Peak times are defined as the time of the highest 10-minute melt rate during a melt event. Deviations were calculated with regard to the average of all three individual lysimeters (i.e. of the snowmelt lysimeter system).

Melt event	Snowmelt lysimeter system		Lysimeter-1		Lysimeter-2		Lysimeter-3	
	Melt rate (mm 10 min ⁻¹)	Peak time (mm/dd/yy hh:mm)	Deviation from avg. melt rate (mm 10 min ⁻¹)	Deviation from avg. peak time (min)	Deviation from avg. melt rate (mm 10 min ⁻¹)	Deviation from avg. peak time (min)	Deviation from avg. melt rate (mm 10 min ⁻¹)	Deviation from avg. peak time (min)
SM-April-a 28.04. 14:30–21:40	0.20	28.04. 16:50	-0.02	33	-0.13	-37	0.16	3
SM-April-b 29.04. 10:50–20:40	1.22	29.04. 15:40	0.08	3	-0.02	-37	-0.06	33
SM-April-c 01.05. 07:50–14:20	1.32	01.05. 11:50	-0.50	-17	-0.20	33	0.70	-16
SM-Nov-a 11.11. 01:30–09:50	0.31	11.11. 04:10	0.05	-20	-0.06	0	0.01	20
SM-Nov-b 16.11. 09:10–17.11. 02:10	0.28	16.11. 18:20	-0.02	-7	0.01	3	0.01	3
SM-Nov-c 21.11. 00:10–22.11. 05:10	0.88	21.11. 20:30	-0.16	-133	0.28	-133	-0.12	266

Spatial and temporal variability of snowmelt during individual melt events measured with the snowmelt lysimeter system

The snowmelt lysimeter system with its three individual lysimeters potentially allows for monitoring the heterogeneous melt-out of the snowpack at the plot scale. To test this, melt rates and peak times of the individual snowmelt lysimeters were compared among each other for six melt events that occurred during the April and November periods. In addition, the individual melt rate measurements were compared against the average melt rates of the entire snowmelt lysimeter system.

Three melt events occurred in April due to rising air temperatures (28 April 14:30–21:40 SM-April-a, 29 April 10:50–20:40 SM-April-b and 1 May 07:50–14:20 SM-April-c). In November, three major snowmelt events were recorded on 11 November from 01:30 to 09:50 (SM-Nov-a), between 16 November 09:10 and 17 November 02:10 (SM-Nov-b) and between 21 November 01:10 and 22 November 05:10 (SM-Nov-c).

Figure 3c and Figure 4c show that for the six snowmelt events, the 10-minute average melt rates were within the range of 0.2 mm (28 April) and 1.32 mm (1 May). The data shown in Table 2 indicate that the deviations from the 10-minute average melt rates can be large, especially during the major melt events. The largest deviations from the 10-minute average melt rates occurred on 1 May (SM-April-c), which were around 0.66 mm for Lysimeter-3 and around -0.45 mm for Lysimeter-1, indicating a high temporal variability of the melt-out from the snowpack. Overall, the three individual lysimeters showed no consistent bias of melt rate measurements. Similar to the melt rates, there was no consistent bias of the peak times of the three individual lysimeters (Table 2). From the six snowmelt events, the 21 November event resulted in the longest offsets of peak times relative to the average (i.e., -133 min for Lysimeters-1 and 2 and 266 min for Lysimeter-3). For the other five events, the temporal offsets were generally much shorter and ranged between -37 min and 33 min.

DISCUSSION: PERFORMANCE OF THE SNOWMELT LYSIMETER SYSTEM

Capturing snowmelt rates

The comparison of the total precipitation and melt rates during the April and November periods showed a good agreement between the snowmelt lysimeter system and the heated rain gauge (Table 1). This suggests that the snowmelt lysimeter system provides a representative estimate of incoming precipitation and naturally occurring snowmelt volume at the plot scale.

The deviations between the 10-minute melt rates from the three individual lysimeters and their average melt rate (i.e. the snowmelt lysimeter system) suggests large spatial and temporal variability of the snowmelt process at the plot scale (Table 2). Additionally, differences in peak times occurred during small- but also high-intensity melt rates. As reported by Kattelmann (2000), unenclosed lysimeters might facilitate lateral flow of meltwater from the surrounding snowpack into the funnel of the individual snowmelt lysimeters. After the snow depth decreases to the ridge of the funnel, however, the unenclosed lysimeter becomes an enclosed lysimeter, which restricts meltwater contribution from the surrounding snowpack (Kattelmann, 2000). Further, snow distribution by wind may affect the amount of snow accumulated on the lysimeter funnel and thus, the snowmelt volume registered by the individual lysimeters.

The unheated precipitation collector significantly underestimated the total precipitation and melt volumes compared to the snowmelt lysimeter system and the heated rain gauge by up to 43% (Table 1). Daily melt rates measured with the unheated precipitation collector were often lower than the respective values from the snowmelt lysimeter system (Figure 6, Figure 7). One of the main reasons for the underestimation of snowmelt with the unheated precipitation collector was the extended funnel that only allowed a restricted snow volume to accumulate. This snow volume was likely to be much smaller than the accumulated snowpack on the ground and thus, the snowmelt from the snow volume in the unheated precipitation collector might not be representative for the snowmelt occurring naturally from the snowpack on the ground. As a result, the smaller amount of snow volume in the extended funnel of the unheated precipitation collector generated outflow more rapidly when air temperature increased. In addition, during high intensity snowfall events, the extended funnel was likely to be filled up completely with snow so that remaining snowfall could not be captured by the unheated precipitation collector. Also, if the air temperature and/or incoming solar radiation were low during snowfall events, the black colour of the extended funnel was not sufficient to accelerate the melt process, and thus the extended funnel might have filled up with snow completely.

Further, wind can cause significant errors of solid precipitation records due to under-catch by around 20%–50% (Rasmussen et al., 2012). In addition, if the extended funnel of the unheated precipitation collector was completely filled with snow, wind was likely to blow off additional incoming snow. Another potential reason for the under-catch of snowmelt in the unheated precipitation collector is evaporation from the snow accumulated in the extended funnel. Long storage times and/or wind gusts reaching into the extended funnel may have en-

hanced evaporation (Nespor and Sevruck, 1999; Earman et al., 2006). Overall, the comparison analysis suggests that the unheated precipitation collector with extended funnel is not applicable for melt rate monitoring at daily temporal resolution.

Capturing the isotopic signature of snowmelt

Figure 6 and Figure 7 show distinct decreases in the meltwater $\delta^{18}\text{O}$ values during the initial snowmelt events on the 1st and 2nd day of the April and November periods. After that, the meltwater $\delta^{18}\text{O}$ values increased continuously over several days until the snowpack was completely melted. Both collection systems captured this general pattern in the isotope values. Figure 5 shows that most snowmelt samples of both collection systems plotted on the approximated local meteoric water line. The three most negative meltwater samples of the November period plotted below the linear regression line, suggesting that isotopic fractionation occurred within the snowpack. Such isotopic fractionation processes may be driven by vapour condensation and (re-)freezing of liquid water resulting in a depletion of the meltwater leaving the snowpack (Ala-aho et al., 2017; Cooper, 1998; Lyon et al., 2010; Rodhe, 1998; Taylor et al., 2001; Unnikrishna et al., 2002). Both sampling systems captured this isotopic response of the early melt period. Since there were no other snowmelt samples that plotted substantially off the linear regression line, we conclude that other kinetic fractionation effects within the two sampling systems (e.g., due to evaporation or sublimation) might be insignificant.

Overall, the isotopic signature of the samples from the unheated precipitation collector was more variable in time during both snowmelt periods compared to the isotopic signature of the samples from the individual snowmelt lysimeters. This can partly be explained with the design of the unheated precipitation collector. The funnel limited the volume of snow to be collected, which resulted in a substantial under-catch compared to the snowmelt lysimeter system and the heated rain gauge (Chapter “Capturing snowmelt rates”). Since the unheated precipitation collector sampled only distinct volume increments of precipitation events, the isotopic variability between the collected samples can potentially be large. In addition, the isotopic composition of incoming precipitation can be highly variable during individual events, (Dansgaard, 1964; McDonnell, 1990; Munksgaard et al., 2012; von Freyberg et al., 2017), which might further intensify this incremental sampling effect of the unheated precipitation collector. The more damped isotopic signature of the lysimeter snowmelt samples can be explained by vertical and lateral mixing of meltwater percolating through the isotopically variable layers of the snowpack. Such mixing processes have been found to depend on the ambient conditions such as incoming solar energy input, temperature of the air and of the ground and layering of the snowpack, as well as on the amount and intensity of incoming precipitation (Lee et al., 2010; Penna et al., 2017; Unnikrishna et al., 2002). Because the snowmelt lysimeter system collected samples from the snowpack that naturally formed on the ground, it integrated the isotopic signature of all snowfall events compared to the unheated precipitation collector with its constrained funnel volume.

During both observation periods, the samples from the unheated precipitation collector were marginally but consistently heavier in $\delta^{18}\text{O}$ compared to the samples from the snowmelt lysimeter system (Figures 6b,c and Figures 7b,c). However, the isotope signal of the meltwater samples from the unheated precipitation collector did not suggest a strong kinetic fractionation effect (i.e., evaporation) in the dual isotope plots as most of

the snowmelt samples plot on the linear regression line (Figure 5). As a consequence, this behaviour can mainly be explained by the incremental sampling effect (more heavy snow was sampled compared to the snowmelt lysimeters system) and simple mixing. Other factors, such as fractionation during phase transitions (sublimation/condensation/evaporation, freeze/melt) are less obvious from our data set (Earman et al., 2006; Kendall and Caldwell, 1998; Taylor et al., 2001).

Our results showed that the isotope signature of the snowmelt samples from the snowmelt lysimeter system was delayed compared to the samples from the unheated precipitation collector. This can be explained by the generally larger snow volume captured by the snowmelt lysimeter system compared to the extended funnel of the unheated precipitation collector. Consequently, under similar ambient conditions, the snowpack on top of the snowmelt lysimeter system requires more time to melt. In addition, the black-coloured extended funnel of the unheated precipitation collector was specifically designed to accelerate the melt process to reduce the exposure time of the meltwater in the funnel. Thus, in order to capture the isotopic signature of natural meltwater from a snowpack on the ground, the snowmelt lysimeter system may provide more representative samples at daily resolution. The unheated precipitation collector, on the other hand, often fails to capture this signature because of accelerated melt and incremental sampling effect. This collection system may, however, still provide a reasonable estimate of the relative day-to-day variability of snowmelt, depending on the purpose of the study.

Both collection systems captured an initial decrease of $\delta^{18}\text{O}$ in meltwater, which was followed by a systematic increase of $\delta^{18}\text{O}$ until the entire snowpack was melted (Figures 6b,c and Figures 7b,c). A possible explanation may be fractionation during re-freezing of the initial meltwater that percolated from the snow surface through the snowpack. As a consequence, the snowpack becomes isotopically heavier, and so does the meltwater draining from this snowpack with progressive melting (Herrmann, 1978; Stichler et al., 1981; Taylor et al., 2001; Unnikrishna et al., 2002). Alternatively, the isotopic signature of the meltwater samples may simply reflect the melt-out of the individual layers of the snowpack that build up during the individual precipitation events. However, we did not measure the isotopic signature of incoming precipitation at the field site, and thus, cannot draw any conclusions about the sources or processes causing the isotope pattern in the daily snowmelt samples.

CONCLUSION

This study compared two snowmelt collection systems with focus on their ability to properly capture snowmelt rates and the isotopic composition of meltwater. A low-cost, unheated precipitation collector (ca. 200 US\$, excluding automatic water sampler) was evaluated against a newly developed snowmelt lysimeter system (ca. 4000 US\$, excluding automatic water sampler) consisting of three individual unenclosed lysimeters. The comparison analysis was carried out for samples from two snowfall-snowmelt periods in April and November 2016.

Although the unheated precipitation collector sampled much less snow than the snowmelt lysimeter system (under-catch of up to 43%), both systems were able to capture very similar isotope patterns during both periods. Thus, despite the substantial under-catch, the low-cost unheated precipitation collector seems sufficient to capture the general isotope signal of snowmelt over the course of a snowfall and snowmelt period. Since the unheated precipitation collector requires only low maintenance and because its automatic water sampler can potentially

be run on battery power, possible areas of applications are at remote locations or at sites where many locations have to be sampled. In order to adequately capture the rates of incoming precipitation (and melt) at a site, an additional heated rain gauge and a temperature logger would have to be installed. The strength of the snowmelt lysimeter system is its ability to capture both the variability in melt rates, as well as the isotopic composition of snowmelt at daily resolution and thus, to provide valuable information about the snowmelt processes at the plot scale. The system is based on standard technical components, and thus can potentially be rebuilt at other sites with moderate effort and costs. Compared to the unheated precipitation collector, the lysimeter system is more cost-intensive and requires more extensive maintenance. In addition, its complex set-up and the high power requirements prohibit an installation of the system at remote locations.

For catchment scale studies that aim at quantifying the fraction of snowmelt in streamflow based on hydrograph separation, other important factors such as topography, vegetation cover and soil depth control the melt process (Schmieder et al., 2016; Unnikrishna et al., 2002). Ongoing research in the Erlenbach and neighbouring catchments focuses on the effects of elevation and vegetation cover on the isotopic evolution of snowmelt. For this, two additional snowmelt lysimeters were installed at a forested site (1185 m a.s.l.) and at another grassland site (1405 m a.s.l.) in December 2016. This extended sampling network of snowmelt lysimeter systems will provide further insights into how landscape and climatic properties control snowmelt and its isotopic evolution.

Acknowledgements. This project is supported by the Swiss National Science Foundation SNF through the Joint Research Projects (SCOPES) Action (Grant IZ73Z0_152506). We thank the staff of the Swiss Federal Institute for Forest, Snow and Landscape Research (WSL), especially Karl Steiner for great support in the field and Alessandro Schlumpf for the sample analysis. We also thank Prof. James Kirchner, Physics of Environmental Systems (ETH), his lab facility staff, Björn Studer, Daniel Meyer for help in the laboratory. We also thank the anonymous reviewers for their valuable suggestions that have helped to improve the manuscript.

REFERENCES

- Ala-aho, P., Tetzlaff, D., Mcnamara, J.P., Laudon, H., Kormos, P., Soulsby, C., 2017. Modeling the isotopic evolution of snowpack and snowmelt: Testing a spatially distributed parsimonious approach. *Water Resour. Res.*, 2404–2418. DOI: 10.1002/2016WR019638.
- Bales, R.C., Davis, R.E., Williams, M.W., 1993. Tracer release in melting snow: diurnal and seasonal patterns. *Hydrol. Process.*, 7, 389–401. DOI:10.1002/hyp.3360070405.
- Barnett, T.P., Adam, J.C., Lettenmaier, D.P., 2005. Potential impacts of a warming climate on water availability in snow-dominated regions. *Nature*, 438, 303–309. DOI: 10.1038/nature04141.
- Beniston, M., 2003. *Climatic Change in Mountain Regions: A Review of Possible Impacts*. 1st Ed. Climatic Change. Kluwer Academic Publishers, Dordrecht. DOI: 10.1023/A:1024458411589.
- Berghuijs, W.R., Woods, R.A., Hrachowitz, M., 2014. A precipitation shift from snow towards rain leads to a decrease in streamflow. *Nat. Clim. Chang.*, 4, 583–586. DOI: 10.1038/NCLIMATE2246.
- Bierkens, M.F.P., van Beek, L.P.H., 2009. Seasonal Predictability of European Discharge: NAO and Hydrological Response Time. *J. Hydrometeorol.*, 10, 953–968. DOI: 10.1175/2009JHM1034.1.
- Burch, V.H., Forster, Felix, Schleppe, P., 1996. Zum Einfluss des Waldes auf die Hydrologie der Flysch-Einzugsgebiete des Alptals. *Schweizerische Zeitschrift für Forstwes. D*, 925–938.
- Clark, I.D., Fritz, P., 1997. *Environmental Isotopes in Hydrogeology*. CRC Press LLC, Florida, USA.
- Cooper, L.W., 1998. *Isotopic Fractionation in Snow Cover, Isotope Tracers in Catchment Hydrology*. Elsevier B.V. DOI: 10.1016/B978-0-444-81546-0.50011-2.
- Dansgaard, W., 1964. Stable isotopes in precipitation. *Tellus*, 16, 436–468. DOI: 10.3402/tellusa.v16i4.8993.
- Dinger, T., Payne, B.R., Florkowski, T., Martinec, J., Tongiorgi, E., 1970. Snowmelt runoff from measurements of tritium and oxygen-18. *Water Resour. Res.*, 6, 110. DOI: 10.1029/WR006i001p00110.
- Earman, S., Campbell, A.R., Phillips, F.M., Newman, B.D., 2006. Isotopic exchange between snow and atmospheric water vapor: Estimation of the snowmelt component of groundwater recharge in the southwestern United States. *Journal of Geophysical Research*, 111, D09302. DOI: 10.1029/2005JD006470.
- Feyen, H., Wunderli, H., Wydler, H., Papritz, A., 1999. A tracer experiment to study flow paths of water in a forest soil. *J. Hydrol.*, 225, 155–167. DOI: 10.1016/S0022-1694(99)00159-6.
- Fischer, B.M.C., Rinderer, M., Schneider, P., Ewen, T., Seibert, J., 2015. Contributing sources to baseflow in pre-alpine headwaters using spatial snapshot sampling. *Hydrol. Process.*, 29, 5321–5336. DOI: 10.1002/hyp.10529.
- Frisbee, M.D., Phillips, F.M., Campbell, A.R., Hendrickx, J.M.H., 2010. Modified passive capillary samplers for collecting samples of snowmelt infiltration for stable isotope analysis in remote, seasonally inaccessible watersheds 1: laboratory evaluation. *Hydrol. Process.*, 24, 7, 825–833.
- Gröning, M., Lutz, H.O., Roller-Lutz, Z., Kralik, M., Gourcy, L., Pöhlstein, L., 2012. A simple rain collector preventing water re-evaporation dedicated for $\delta^{18}\text{O}$ and $\delta^2\text{H}$ analysis of cumulative precipitation samples. *J. Hydrol.*, 448–449, 195–200. DOI: 10.1016/j.jhydrol.2012.04.041.
- Haupt, H., 1969. A Simple Snowmelt Lysimeter. *Water Resour. Res.*, 5, 3, 714–718.
- Hegg, C., McArdeell, B.W., Badoux, A., 2006. One hundred years of mountain hydrology in Switzerland by the WSL. *Hydrol. Process.*, 20, 371–376. DOI: 10.1002/hyp.6055.
- Helvey, J.D., Fowler, W.B., 1980. A new method for sampling snow melt and rainfall in forests. *JAWRA Journal of the American Water Resources Association*, 16, 5, 938–940.
- Herrmann, A., 1978. A recording snow lysimeter. *J. Glaciol.*, 20, 82, 209–213.
- Hooper, R.P., Shoemaker, C.A., 1986. A comparison of Chemical and Isotopic Hydrograph Separation. *Water Resour. Res.*, 22, 1444–1454. DOI: 10.1029/WR022i010p01444.
- Huth, A.K., Leydecker, A., Sickman, J.O., Bales, R.C., 2004. A two-component hydrograph separation for three high-elevation catchments in the Sierra Nevada, California. *Hydrol. Process.*, 18, 1721–1733. DOI: 10.1002/hyp.1414.
- Juras, R., Pavlásek, J., Vitvar, T., Šanda, M., Holub, J., Jankovec, J., Linda, M., 2016. Isotopic tracing of the outflow during artificial rain-on-snow event. *J. Hydrol.*, 541, 1145–1154. DOI: 10.1016/j.jhydrol.2016.08.018.
- Kattelmann, R., 2000. Snowmelt lysimeters in the evaluation of snowmelt models. *Ann. Glaciol.*, 31, 406–410. DOI: 10.3189/172756400781820048.
- Kendall, C., Caldwell, E., 1998. Chapter 2: Fundamentals of Isotope Geochemistry, *Isotope Tracers in Catchment Hydrology*. Elsevier B.V. doi:http://dx.doi.org/10.1016/B978-0-444-81546-0.50009-4.
- Klaus, J., McDonnell, J.J., 2013. Hydrograph separation using stable isotopes: Review and evaluation. *J. Hydrol.*, 505, 47–64. DOI: 10.1016/j.jhydrol.2013.09.006.
- Laudon, H., 2004. Hydrological flow paths during snowmelt: Congruence between hydrometric measurements and oxygen 18

- in meltwater, soil water, and runoff. *Water Resour. Res.*, 40, 1–9. DOI: 10.1029/2003WR002455.
- Laudon, H., Hemond, H.F., Krouse, R., Bishop, K.H., 2002. Oxygen 18 fractionation during snowmelt: Implications for spring flood hydrograph separation. *Water Resour. Res.*, 38, 11, 1–10. DOI: 10.1029/2002WR001510.
- Lee, J., Feng, X., Faiia, A.M., Posmentier, E.S., Kirchner, J., Osterhuber, R., Taylor, S., 2010. Isotopic evolution of a seasonal snowcover and its melt by isotopic exchange between liquid water and ice. *Chem. Geol.*, 270, 126–134. DOI: 10.1016/j.chemgeo.2009.11.011.
- Lyon, S.W., Laudon, H., Seibert, J., Mörth, M., Tetzlaff, D., Bishop, K.H., 2010. Controls on snowmelt water mean transit times in northern boreal catchments. *Hydrol. Process.*, 24, 1672–1684. DOI: 10.1002/hyp.7577.
- Martinec, J., 1987. Meltwater percolation through an alpine snowpack. In: *Proc. Avalanche Formation, Movement and Effects*. (Davos Symposium, September 1986). IAHS Publ. no. 162. IAHS, Wallingford, pp. 255–264.
- McDonnell, J.J., 1990. A rational for old water discharge through macropores in a steep, humid catchment. *Water Resour. Res.*, 26, 2821–2832. DOI: 10.1029/WR026i011p02821.
- Munksgaard, N.C., Wurster, C.M., Bass, A., Bird, M.I., 2012. Extreme short-term stable isotope variability revealed by continuous rainwater analysis. *Hydrol. Process.*, 26, 3630–3634. DOI: 10.1002/hyp.9505.
- Nespor, V., Sevruk, B., 1999. Estimation of wind-induced error of rainfall gauge measurements using a numerical simulation. *J. Atmospheric Ocean. Technol.*, 16, 450–464.
- Obled, C., Rosse, B., 1977. Mathematical models of a melting snowpack at an index plot. *J. Hydrol.*, 32, 139–163. DOI: 10.1016/0022-1694(77)90123-8.
- Penna, D., Ahmad, M., Birks, S.J., Bouchaou, L., Brenčić, M., Butt, S., Holko, L., Jeelani, G., Martínez, D.E., Melikadze, G., Shanley, J.B., Sokratov, S.A., Stadnyk, T., Sugimoto, A., Vreča, P., 2014a. A new method of snowmelt sampling for water stable isotopes. *Hydrol. Process.*, 28, 5637–5644. DOI: 10.1002/hyp.10273.
- Penna, D., Engel, M., Mao, L., Dell’Agnese, A., Bertoldi, G., Comiti, F., 2014b. Tracer-based analysis of spatial and temporal variation of water sources in a glacierized catchment. *Hydrol. Earth Syst. Sci. Discuss.*, 11, 4879–4924. DOI: 10.5194/hessd-11-4879-2014.
- Penna, D., Engel, M., Bertoldi, G., Comiti, F., 2017. Towards a tracer-based conceptualization of meltwater dynamics and streamflow response in a glacierized catchment. *Hydrol. Earth Syst. Sci.*, 21, 23–41. DOI: 10.5194/hess-2016-334.
- Rasmussen, R., Baker, B., Kochendorfer, J., Meyers, T., Landolt, S., Fischer, P.A., Black, J., Thériault, J.M., Kucera, P., Gochis, D., Smith, C., Nitu, R., Hall, M., Ikeda, K., Gutmann, E., 2012. How Well Are We Measuring Snow? *Am. Meteorol. Soc.*, 811–829. DOI: 10.1175/BAMS-D-11-00052.1.
- Rodhe, A., 1998. Chapter 12 – Snowmelt-Dominated Systems, *Isotope Tracers in Catchment Hydrology*. Elsevier B.V. DOI: 10.1016/B978-0-444-81546-0.50019-7.
- Šanda, M., Kulasov, A., Milena, C., 2010. Runoff formation in a small catchment at hillslope and catchment scales. *Hydrol. Process.*, 2256, 2248–2256. DOI: 10.1002/hyp.7614.
- Šanda, M., Vitvar, T., Kulasová, A., Jankovec, J., Císlarová, M., 2014. Run-off formation in a humid, temperate headwater catchment using a combined hydrological, hydrochemical and isotopic approach (Jizera Mountains, Czech Republic). *Hydrol. Process.*, 3229, 3217–3229. DOI: 10.1002/hyp.9847.
- Schmieder, J., Hanzer, F., Marke, T., Garvelmann, J., Warscher, M., Kunstmann, H., Strasser, U., 2016. The importance of snowmelt spatiotemporal variability for isotope-based hydrograph separation in a high-elevation catchment. *Hydrol. Earth Syst. Sci.*, 20, 5015–5033. DOI: 10.5194/hess-20-5015-2016.
- Shanley, J.B., Sundquist, E.T., Kendall, C., 1995. *Water, Energy, and Biochemical Budget Research At Sleepers River Research Watershed*, Vermont. U.S. Geological Survey, Bow, New Hampshire.
- Singla, S., Céron, J.P., Martin, E., Regimbeau, F., Déqué, M., Habets, F., Vidal, J.P., 2012. Predictability of soil moisture and river flows over France for the spring season. *Hydrol. Earth Syst. Sci.*, 16, 201–216. DOI: 10.5194/hess-16-201-2012.
- Stähli, M., Gustafsson, D., 2006. Long-term investigations of the snow cover in a subalpine semi-forested catchment. *Hydrol. Process.*, 20, 411–428. DOI: 10.1002/hyp.6058.
- Staudinger, M., Seibert, J., 2014. Predictability of low flow – An assessment with simulation experiments. *J. Hydrol.*, 519, 1383–1393. DOI: 10.1016/j.jhydrol.2014.08.061.
- Stewart, I.T., 2009. Changes in snowpack and snowmelt runoff for key mountain regions. *Hydrol. Process.*, 23, 1, 78–94. DOI: 10.1002/hyp.7128.
- Stichler, W., Rauert, W., Martinec, J., 1981. Environmental isotope studies of an alpine snowpack. *Nord. Hydrol.*, 12, 297–308.
- Taylor, S., Feng, X., Kirchner, J.W., Osterhuber, R., 2001. Isotopic evolution of a seasonal snowpack and its melt. *Water Resour. Res.*, 37, 759–769.
- Taylor, S., Feng, X., Renshaw, C.E., Kirchner, J.W., 2002a. Isotopic evolution of snowmelt 2. Verification and parameterization of a one-dimensional model using laboratory experiments. *Water Resour. Res.*, 38, 10. DOI: 10.1029/2001WR000815.
- Taylor, S., Feng, X., Williams, M., Mcnamara, J., 2002b. How isotopic fractionation of snowmelt affects hydrograph separation. *Hydrol. Process.*, 3690, 3683–3690. DOI: 10.1002/hyp.1232.
- Tekeli, A.E., Şorman, A.A., Şensoy, A., Şorman, A.Ü., Bonta, J., Schaefer, G., 2005. Snowmelt lysimeters for real-time snowmelt studies in Turkey. *Turkish J. Eng. Environ. Sci.*, 29, 29–40.
- Unnikrishna, P. V., McDonnell, J.J., Kendall, C., 2002. Isotope variations in a Sierra Nevada snowpack and their relation to meltwater. *J. Hydrol.*, 260, 38–57.
- von Freyberg, J., Studer, B., Kirchner, J.W., 2017. A lab in the field: high-frequency analysis of water quality and stable isotopes in stream water and precipitation. *Hydrol. Earth Syst. Sci.*, 21, 1721–1739. DOI: 10.5194/hess-21-1721-2017.
- Würzer, S., Wever, N., Juras, R., Lehning, M., Jonas, T., 2017. Modelling liquid water transport in snow under rain-on-snow conditions – considering preferential flow. *Hydrol. Earth Syst. Sci.*, 21, 1741–1756. DOI: 10.5194/hess-21-1741-2017.
- Zappa, M., Bernhard, L., Fundel, F., Jörg-Hess, S., 2012. Vorhersage und Szenarien von Schnee- und Wasserressourcen im Alpenraum. *Forum für Wissen* 19–27.

Received 3 July 2017
Accepted 9 December 2017

APPENDIX

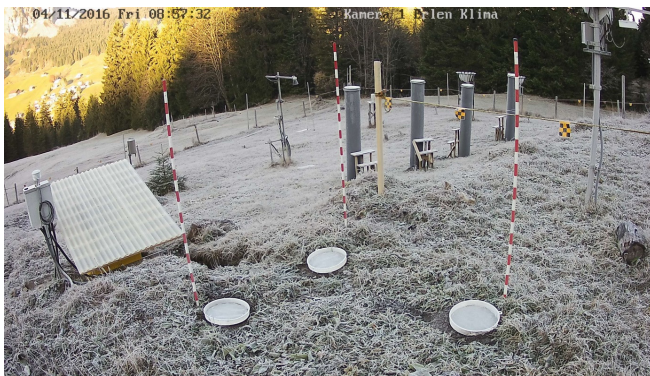


Fig. A1. Webcam picture before the snowfall event in November 2016 (04.11.2016 08:57).

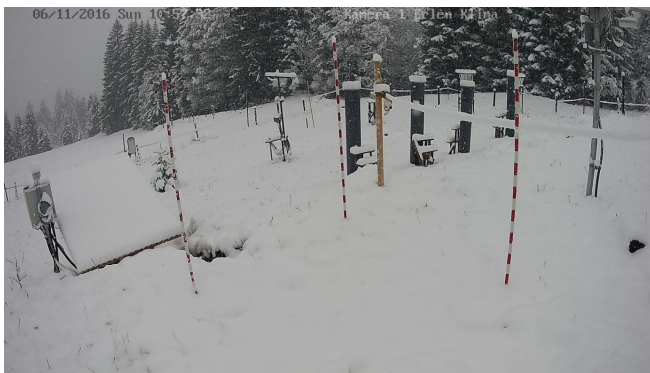


Fig. A2. Webcam picture during the snowfall event in November 2016 (06.11.2016 10:57).



Fig. A3. Unheated precipitation collector with extended funnel connected to the 6712-Teledyne Isco automatic water sampler during the winter season 2015/16.

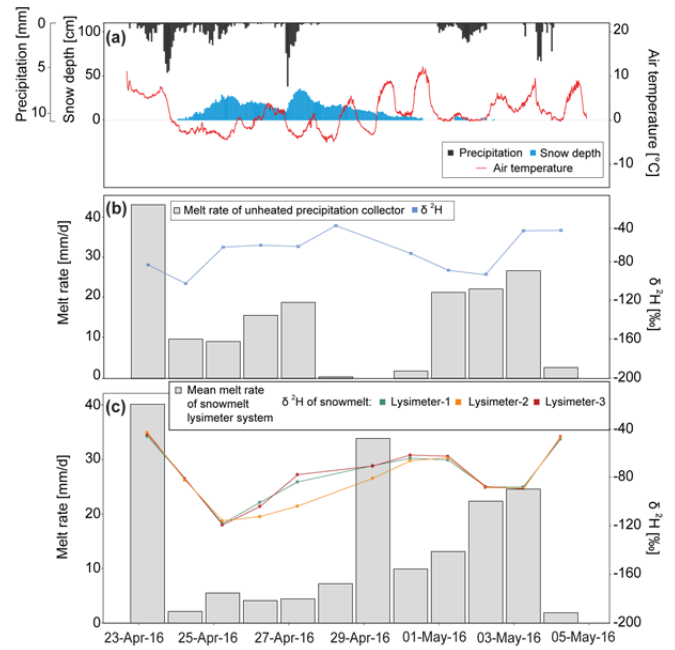


Fig. A4. The snowfall-snowmelt period in April 2016. (a) Precipitation and snow depth (left axis) as well as air temperature (right axis) at the field site Erlenhöhe. (b) Daily meltwater sample volume (left axis) and $\delta^2\text{H}$ values (right axis) from the unheated precipitation collector with extended funnel. (c) Daily meltwater sample volume (left axis) and $\delta^2\text{H}$ values (right axis) from the snowmelt lysimeter system.

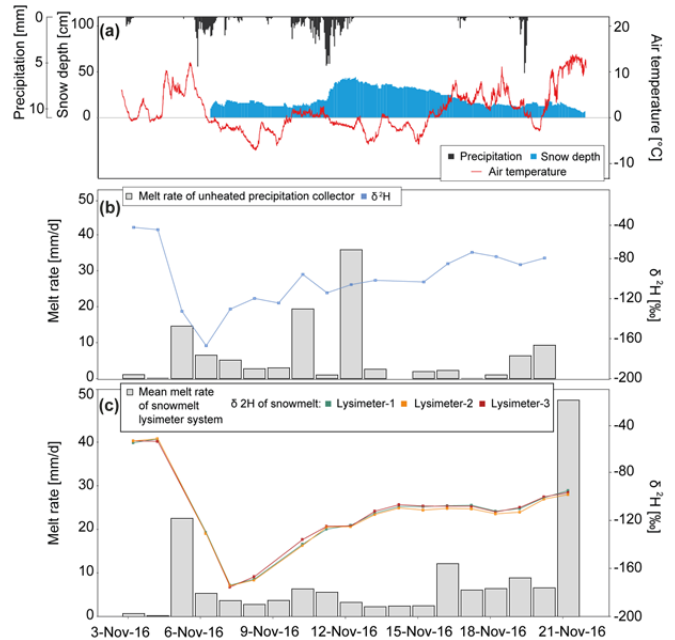


Fig. A5. The snowfall-snowmelt period in November 2016. (a) Precipitation and snow depth (left axis) as well as air temperature (right axis) at the field site Erlenhöhe. (b) Daily meltwater sample volume (left axis) and $\delta^2\text{H}$ values (right axis) from the unheated precipitation collector with extended funnel. (c) Daily meltwater sample volume (left axis) and $\delta^2\text{H}$ values (right axis) from the snowmelt lysimeter system.